Broadband polarizer using single-layer grating with ultra-high extinction ratio

Cite as: AIP Advances 13, 055003 (2023); doi: 10.1063/5.0135669
Submitted: 28 November 2022 • Accepted: 12 April 2023 •
Published Online: 2 May 2023

Chunhua Qin,[1] Yiyuan Wang,[1] Ziying Liu,[1] Wenjia Li,[1,a)] Yuxiang Li,[1] Ping Li,[1] Zheng Zhu,[1] Chunying Guan,[1] Jinhui Shi,[1,2,b)] and Kenneth T. V. Grattan[3]

AFFILIATIONS

[1] Key Laboratory of In-Fiber Integrated Optics of Ministry of Education, College of Physics and Optoelectronic Engineering, Harbin Engineering University, Harbin 150001, China
[2] National Key Laboratory of Underwater Acoustic Technology, Harbin Engineering University, Harbin 150001, China
[3] School of Science & Technology, City, University of London, Northampton Square, London EC1V 0HB, United Kingdom

[a)] liwenjia@hrbeu.edu.cn
[b)] **Author to whom correspondence should be addressed:** shijinhui@hrbeu.edu.cn

ABSTRACT

Polarizers are an essential optical element for tailoring the polarization state of electromagnetic waves in a wide range of optical devices. Such polarizers, which exhibit a wide operating bandwidth and high performance, are attracting increasing attention, due to their extensive prospects for use in applications ranging from polarization imaging, to optical communications and detection, among others. However, achieving both broadband performance and ultra-high extinction ratio (ER), and that simultaneously, is still challenging in the design of effective polarizers. To tackle that demand, in this work, an Au-on-silica grating structure has been proposed as the basis of the design of a miniaturized high-efficiency polarizer that practically can cover the entire visible and near-infrared spectral ranges. The single-layer polarizer thus designed can show an ER of 60 dB in this spectral domain, and it has been shown that the geometrical parameters selected have a significant effect on the performance characteristics of the polarizer. Furthermore, an ER of ~150 dB could be achieved merely by regulating the thickness of the grating to achieve the optimum performance. By integrating the high-performance polarizer proposed in this work with an optical fiber "meta-tip," a refractive polarizer with a value of the ER of >45 dB, and that over the entire spectral domain considered, has been demonstrated. Such an approach offers an alternative route to achieving a broadband, powerful, and flexible processing polarizer design.

I. INTRODUCTION

Polarization, as a key property of electromagnetic waves, plays a crucial role in both exploring and controlling the interaction between light and matter. Polarizers are indispensable optical elements to control the polarization properties and thus convert electromagnetic waves with random electric oscillation components into a beam with a particular, usually known polarization, suitable for applications where it is important to provide flexible and precise control of the polarization characteristics of a light beam. For example, a linear polarizer device can directly generate a specific linear polarization needed for a particular application—with such a device having a variety of applications in polarization imaging, optical communications, optical detection, and a wide variety of other fields.[1–9] A key feature, however, in selecting the desired polarization in any optical communication system is both the efficiency and the bandwidth available from nanoscale linear polarizers.

Conventional polarizers mostly rely for their operation on the birefringence of anisotropic materials[10] or nanostructures.[11,12] Recent papers have discussed the various planar arrays of meta-atoms, holes, and other structures (with a subwavelength period) used to allow efficient selection of a particular polarization of linearly polarized light.[9,13–31] To do so, a grating structure consisting of silicon nitride, titanium dioxide, and silicon has been proposed to

achieve a guided-mode resonance polarizer operating near a wavelength of 1550 nm.[21] An ultra-high value of the extinction ratio (ER) of 113 dB at a single wavelength of 1550 nm[22] was obtained by use of an asymmetric polarizer based on surface–plasmon interference. Unfortunately, such designs of polarizers could not offer broadband performance, and thus in attempting to improve polarizer performance, Hemmati *et al.* demonstrated a silicon grating with an ER of ~50 dB, operating over the telecommunications band, with a bandwidth of 50 nm and using guided-mode resonance.[23] Wang *et al.* have fabricated a single-layer gold grid that enabled them to realize a value of ER of 30 dB, over the near-infrared spectral range.[24] A high-efficiency resonant polarizer based on a crystalline silicon-on-quartz material that showed an ER of 35 dB, across a bandwidth of ~110 nm has been reported and operating in the visible region.[25] Iwanaga *et al.* also introduced a polarizer with a II-shape structure, composed of gold material, with an ER value of 41 dB, working the near-infrared spectral range.[26]

When compared to the different types of polarizers available today, the fiber polarizer is more flexible and versatile for use in a wide variety of optical system. Recently, polarizers deposed on the end of an optical fiber or on the fiber cladding (when coated using a nanostructure material) have drawn increasing attention.[13,32–40] For example, Abdullah *et al.* have proposed a Bragg grating-based in-fiber polarizer, which showed an ER value of 20 dB.[13] Furthermore, Yan *et al.* have reported an in-fiber linear polarizer, designed by embedding a 45° tilted fiber grating structure in a fiber spindle, which offered an ER value of 46 dB, at a wavelength close to 1550 nm.[32] Better performance was achieved from a fiber cladding coated with a three-layer film, consisting of an MgF_2 buffer layer, chromium, and gold, allowing high-efficiency polarizer performance, with an enhanced ER value of 256 dB.[36] A fiber polarizer based on a thin silver layer coating on the inner surface of two opposite air holes of a large-core suspended-core fiber has been proposed for an experimental device, achieving an ER of ~20 dB.[37] However, it can be noted that the use of nanostructured fiber polarizers in the fibers or their cladding increase the complexity of the device fabrication and thus limits the range of their practical applications. In contrast, the use of a polarizer on the surface of the fiber can be more easily compatible with readily available processing equipment.[39,40] A wideband fiber in-line polarizer, with a limited ER value, has been demonstrated through the use of an Au nano-grid, fabricated on a single mode optical fiber end face,[39] which was reported to achieve ER values of 20.5 and 15.6 dB at wavelengths of 1550 and 1310 nm, respectively. Moreover, the maximum value of the ER (of ~20 dB) was observed when the device was fabricated by milling a diffraction grating on the fiber facet—however, such a design unfortunately does not show broadband characteristics.[40] Therefore, the challenge has been to realize a grating polarizer on the surface of a fiber, with both a high value of the ER and simultaneous broadband capability. To date, most of the polarizers demonstrated to suffer from a narrow bandwidth and a limited value of ER, as is illustrated in Table I for a range of published data, over the period from 2017. With the demand for polarizers in a variety of communications applications, it is necessary to investigate high-performance broadband polarizers, which demonstrate both ultra-high ER and flexible integration with optical fibers.

In this paper, the design and performance of an Au-on-silica grating structure, covering almost the entire visible and near-infrared spectral range, has been introduced to create a new type of high-efficiency, refractive linear polarizer. In this work, the value of the ER can reach ~100 dB, as the width of the subwavelength grating approaches its period. Furthermore, the ER can be raised to 150 dB by increasing the thickness of the grating. In particular, the use of optical fiber "meta-tip," integrating the polarizer proposed, exhibits an ER surpassing 45 dB, seen over the entire spectral domain considered. Such polarizers, with a readily available single-layer subwavelength grating and offering high performance, serve as polarization selection components—a means ultimately to simplify the complexity of the optical devices in which they are used, and substantially to reduce the difficulty in processing in such systems. This work as a result opens up a novel route to the desired goal of a polarizer with an extremely high ER in the optical spectral range and which could be directly integrated into an optical fiber.

II. METHOD AND RESULTS

Grating is an easy-to-fabricate and multifunctional nanostructure, which are known to enable polarization selection,[14–17,19–29,31] imaging,[19] sensing,[41] and optical focusing,[9] for example. The single-layer subwavelength grating polarizer deposited on a glass substrate, which is proposed in this work, is shown in Fig. 1. The horizontal period, p, of the structure has

TABLE I. Published data on a number of polarizers reported in the literature. D/M: dielectric/metal; S/E: simulation/experiment; T: transmittance; and ER: extinction ratio.

Year	Reference	D/M	Layer	S/E	On-fiber	T	Bandwidth (nm)	ER (-dB)
2017	26	M	1	S	No	0.6	1300–1600	−41
2019	24	M	1	S	No	0.8	1000–2000	−30
2019	23	D	4	E	No	0.98	1550–1600	−50
2020	25	D	1	S	No	0.9	600–700	−50
			4	E	No	<0.7	570–680	−35
2020	19	M	2	S	No	0.9	1400–1900	−42
2021	13	D	1	E	Yes	0.75	1552–1557	−20
···	This work	M	1	S	No	0.7	834–2000	<−66
					Yes		649–2000	−45

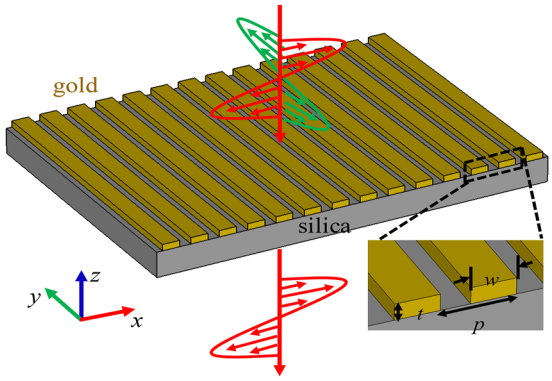

FIG. 1. Schematic diagram of the polarizer design proposed in this work. The geometrical parameters of the subwavelength grating are given as t = 250 nm, w = 120 nm and p = 200 nm.

been set to a value of 200 nm, with the thickness, t, and the width, w, of the gold grating being 250 and 120 nm, respectively. The depth of the substrate was chosen to be 200 nm. The parameters of the gold can be modeled from the experimental data obtained.[42] The refractive index of the substrate SiO_2 layer used was 1.4681. The 3D full-wave numerical simulations (CST Microwave Studio) have been used to investigate the optical properties. The periodic boundary conditions along the x and y directions were used to simulate an infinite structure. The open boundary was used along the z-direction.

The dispersion coefficient spectrum obtained from the gold grating proposed in this work is shown in Fig. 2(a) for both x- and y-polarized light, with normal incidence. Here, T_i, R_i, and A_i represent the transmission intensity, reflection intensity, and absorption intensity, respectively. Intuitively, the transmission intensity of the x-polarized light will be much greater than that of the y-polarized light where the transmission intensity of the y-polarized light is always close to zero in the band discussed, and which can guarantee both broadband performance and an ultra-high value of the ER. By contrast, the transmission intensity of the x-polarized light is mostly >0.5, with a bandwidth of 1342 nm, and the value exceeds 0.7 across a bandwidth of 1303 nm. Figure 2(b) shows an ER value of the gold grating polarizer, calculated by using a relationship where ER = $-10^*\lg(T_x/T_y)$. The value of the ER can be maintained at >20 dB

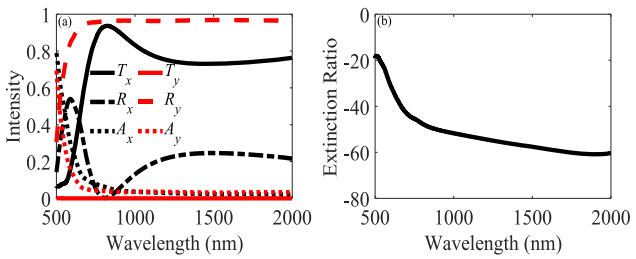

FIG. 2. (a) Intensity spectra of the polarizer for the x-polarized light and y-polarized incident light, along the forward propagation direction (the z axis). (b) ER spectrum of the gold grating polarizer.

over the entire wavelength band, and, in addition, a value >40 dB can be easily realized over the wavelength band of 1335 nm, with a >0.5 transmittance value. The maximum value of ER (61 dB) was obtained for a wavelength of 1901 nm.

In order to further improve the performance of the gold grating polarizer proposed, it is necessary to explore the dependence of the value of the ER on the width of the grating, w. Figure 3(a) shows the transmission intensity with x-polarized incidence when the width w varies from 0 to 200 nm. The overall trend seen shows that the transmitted intensity of the x-polarized light becomes weaker over the wavelength band considered as the width, w, increases. However, when the value of w > 120 nm, the strong transmission intensity bandwidth of the grating design proposed becomes narrowed and redshifts gradually reach zero over the whole wavelength band. The ER spectrum of the polarizer proposed, which is shown in Fig. 3(b), is a function of the width, and the ER peak at the longer wavelengths extends to ~100 dB, but doing so sacrifices the grating strength. Furthermore, the bandwidth of the larger value of the ER expands, with increasing width, w. Figures 3(c) and 3(d) describe the transmission spectra of the x-polarized light and the evolution of the ER, when the values of the width, w, are 60, 120, and 180 nm respectively, corresponding to the black solid, blue dashed-dotted, and red dotted lines, respectively, in Figs. 3(a) and 3(b). When the width w has a value of 180 nm, the ER performance will reach a maximum value (of close to 100 dB) at a wider bandwidth and degrade as the width is reduced to 60 nm. Any particular performance of the ER could be easily designed into the device, by changing the width appropriately over the range from 0 to 200 nm. It is worth noting that the performance of the grating polarizer (in terms of the ER value) maintains its high selectivity and wide bandwidth (but with unsatisfactory transmission intensity) when the value of the width, w, is close to the period of the grating structure proposed.

The effect of the grating height, t, on the transmission intensity and ER performance is now considered. Figures 4(a) and 4(b) show the dependence of the transmission intensity and the ER performance, with x-polarized incidence, on the height, t, as it varies from 50 to 650 nm. The transmission spectrum evolves alternately as the height, t, increases, an effect that may be introduced by using a Fabry–Pérot (F–P) resonance.[43,44] Besides that, a high transmission intensity can be achieved (except for wavelengths <600 nm). There is a hierarchical evolution of the ER performance as a function of the grating height, t, over the wavelength range from 600 to 2000 nm (which is similar to the phenomena that also exist in a reflective grating structure[45]). As the value of t increases, the ER peak could rise to be close to ~150 dB within the wavelength band considered. A theoretical model can be used to analyze the mechanism of the enhanced transmission, as follows. The surface plasmon polaritons (SPPs) are seen in the inset of Fig. 4(b), which could be excited beside adjacent unit when the following condition is met:[46]

$$k_{spp} = k_0\sqrt{\frac{\varepsilon_d\varepsilon_m}{\varepsilon_d + \varepsilon_m}}, \tag{1}$$

where k_0 and k_{spp} refer to the wave vector of the incident light and the SPP, respectively. The permittivity of the metal and the dielectric material can be represented by ε_m and ε_d, respectively. The wavelength of the SPP, given by λ_{spp}, can be written as follows:

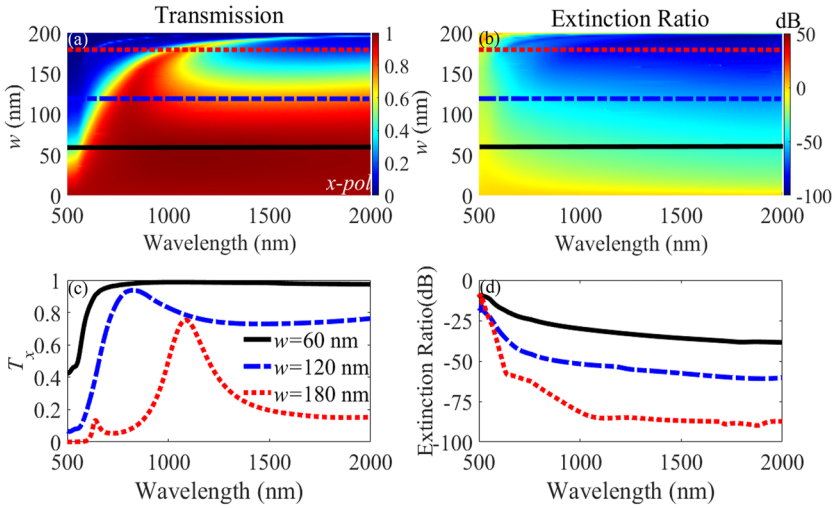

FIG. 3. (a) Dependence of the transmission spectra of the polarizer at the *x*-polarized incidence on the grating width, *w*. (b) Dependence of ER spectra of the polarizer on the grating width, *w*. (c) The transmission spectra of the polarizer at the *x*-polarized incidence when *w* is given by 60, 120 and 180 nm. (d) ER spectra of the polarizer when *w* is given by 60, 120 and 180 nm.

$$\lambda_{spp} = 2\pi/k_{spp}. \tag{2}$$

According to F–P resonance theory,[47] the distance of the adjacent transmission peak, Δt, can be simplified to be

$$\Delta t \approx \lambda_{spp}/2. \tag{3}$$

Under the above-mentioned condition, the transmission with *x*-polarized incidence can be enhanced where the incident wavelength is set to be 820 nm to explore the enhancement mechanisms. The calculated value of λ_{spp} is 642 nm (Δt is 321 nm, in theory). The simulated distance Δt is about 320 nm that can be calculated according to the values marked by the solid blue (t = 570 nm) and orange dots (t = 250 nm) in Fig. 4(a), which is consistent with the theoretical result. In order to visualize the surface plasmon polaritons excited by the grating structure, the electric field of the grating height t = 600 nm is given in the inset of Fig. 4(b).[46,47] The phenomenon has been caused by the SPP excited by the upper end face of the grating and the air and the F–P resonance between the metal gratings.

Additionally, the bandwidth of ER can always remain broadband, as the gold grating height, *t*, of the proposed structure varies. Figures 4(c) and 4(d) depict the transmission spectra of the *x*-polarized light incidence and the ER evolution when the height, *t*, has been given by 150, 250, and 350 nm—this corresponding to the black solid, blue dashed-dotted, and red dotted lines, respectively [as shown in Figs. 4(a) and 4(b)]. The trends of the transmission intensity with the height, *t*, of 150, 250, and 350 nm are analogous, which can be seen in Fig. 4(c). However, the performance of the ER value differs (by nearly 20 dB), with the variation in height *t* of 150, 250 and 350 nm seen in Fig. 4(d). When the height *t* was assumed to be 350 nm, the value of ER obtained is >60 dB, with a bandwidth approaching 1292 nm from 708 to 2000 nm. As can be seen, the performance of the value of ER could be easily tuned by changing the height, *t*, over the range from 50 to 650 nm.

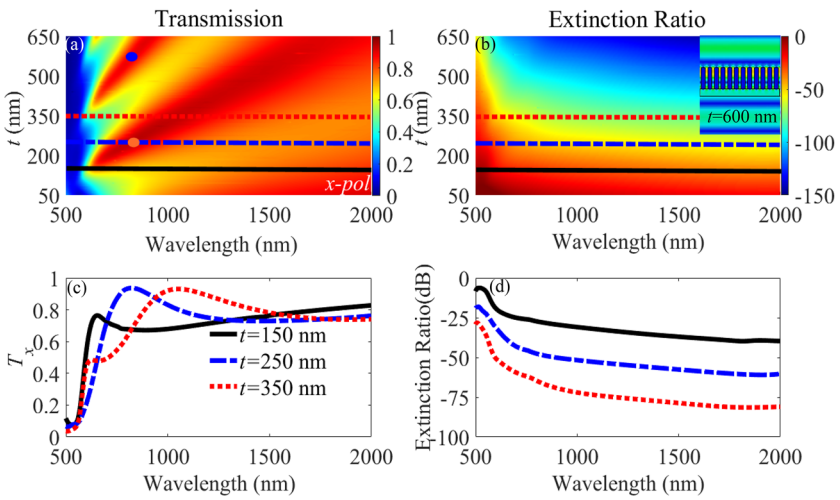

FIG. 4. (a) Transmission spectra of the polarizer at *x*-polarized incidence as a function of the subwavelength grating height, *t*. (b) ER spectra of the polarizer as a function of the subwavelength grating height, *t*. (c) The transmission spectra of the polarizer at the *x*-polarized incidence when *t* is given by 150, 250 and 350 nm (d) ER spectra of the polarizer when *t* is given by 150, 250 and 350 nm. The thickness difference of two adjacent transmission band can be calculated according to the values marked by the blue and orange solid dots.

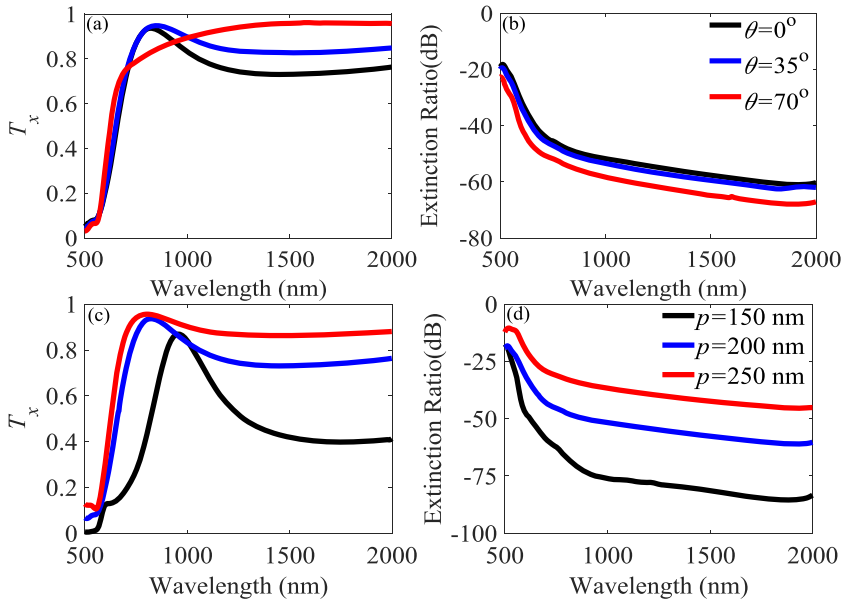

FIG. 5. (a) Transmission spectra of the polarizer at the *x*-polarized incidence when θ is given by 0°, 35° and 70°. (b) ER spectra of the polarizer when θ is given by 0°, 35° and 70°. (c) The transmission spectra of the polarizer at the *x*-polarized incidence when *p* is given by 150, 200 and 250 nm. (d) ER spectra of the polarizer when the value of *p* is 150, 200 and 250 nm.

The effects of the incident angle, θ, and the grating period, *p*, on the transmission intensity of the *x*-polarized incidence and the performance of the ER are also explored here. Figures 5(a) and 5(b) show the transmission intensity and the performance of the ER when the incident angle θ is set to 0°, 35°, and 70° sequentially. When θ is given by 0° or 35°, the performance of the ER can be seen to be approximately the same, but the transmission intensity of the *x*-polarized light is slightly different. However, the transmission intensity of the *x*-polarized light and ER performance are all enhanced as θ reaches 70°. In addition, high-efficiency in the ER value, over the wavelength band considered, could be achieved. Thus, the grating period emerges as having a distinct effect on the transmission intensity of the *x*-polarized light and the ER performance [as shown in Figs. 5(c) and 5(d)]. When the grating period *p* is given by 150, 200, and 250 nm (corresponding to the black, blue, and red solid lines), the trends of the transmission intensity of the *x*-polarized light are analogous, but distinguished in terms of the transmission intensity, an effect that can be seen from Fig. 5(c). Furthermore, Fig. 5(d) shows that the ER performance varies with the grating period *p*. Thus, when the grating period, *p*, is given by 250 nm, an ER value of 75 dB can be obtained (at a wavelength of 940 nm). Consequently, due to the stable broadband and dominant ER performance, such a gold grating polarizer design proposed here has significant potential for use in fiber-integrated devices.

A schematic diagram of the fiber-integrated high-performance polarizer, combined with the proposed single-layer gold grating, is shown in Fig. 6. The gold grating period, *p*, has been set to be 200 nm, and the thicknesses, *t*, and width, *w*, of the gold grating are 250 and 120 nm, respectively, which are the same geometrical parameters as for the grating proposed earlier. The integrated grating polarizer discussed has been based on a Corning SMF-28 single-mode fiber, where the simulation has been carried out using the Finite Difference Time Domain (FDTD) method. The relevant parameters used

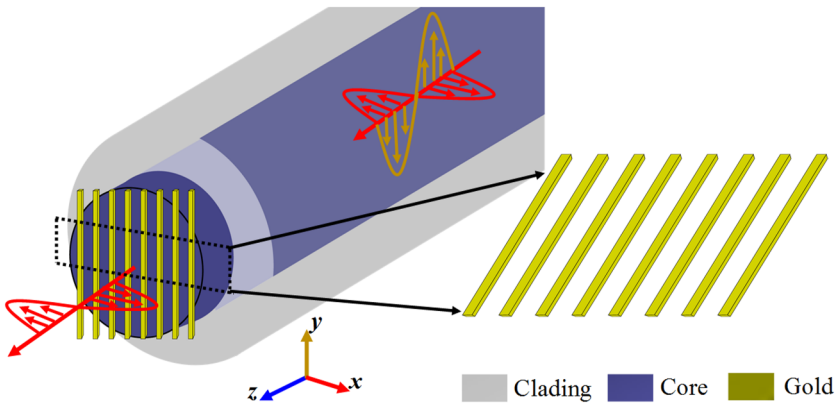

FIG. 6. Schematic diagram of the fiber integrated polarizer. The geometrical parameters of subwavelength grating are the same as the geometrical parameters of subwavelength grating mentioned above. A single-mode fiber with a core diameter of 8 μm, a refractive index of 1.4681, a fiber diameter of 125 μm, and a fiber cladding refractive index of 1.4628 are considered here.

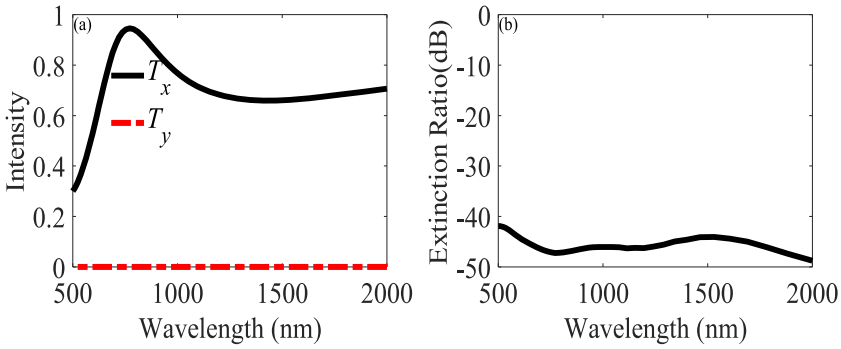

FIG. 7. (a) Intensity spectrum of the polarizer at the *x*-polarized and *y*-polarized light on the fiber end (b) ER of the fiber integrated polarizer.

in that simulation are as follows: the diameter and the refractive index of the core are 8 μm and 1.4681, respectively, and the diameter and the refractive index of the cladding is 125 μm and 1.4628, respectively. To match as close as possible to the situation of light transmission in the fiber, a Gaussian beam with a waist radius of 5 μm has been chosen as the light source in this instance. Compared with the case of a gold grating covering the core only, the fiber end face is too large (which will result in a heavy simulation calculation load). In order to simplify the calculation, the simulation area set here mainly concentrates in the area near the fiber core. The simulation meshing lattice size is 0.02 μm. Therefore, the perfectly matched layer boundary conditions are used along the *x* and *y* directions to absorb unnecessary light.

The transmission spectra of the fiber-integrated grating polarizer, under *x*- and *y*-polarized incidence beams, are shown in Fig. 7(a). Intuitively, the transmission intensity of the *x*-polarized light is much greater than that of the *y*-polarized light. The transmission intensity of the *y*-polarized light always approaches zero in the wavelength band discussed to guarantee both broadband and ultra-high value of the ER. Figure 7(b) similarly depicts the calculated value of the ER of the fiber-integrated gold grating polarizer, obtained using ER = $-10^{*}\lg\,(T_x/T_y)$. ER can then clearly exceed a value of 45 dB over the entire band under consideration. The above discussion has enabled the appropriate parameters of the fiber-integrated polarizers that maintain both the ultra-high ER and near full bandwidth.

III. CONCLUSIONS

In summary, an Au-on-silica grating structure covering practically the entire visible and near-infrared spectral range for a miniaturized and high-efficiency polarizer has been proposed and discussed. Based on a single layer grating, an ER of 60 dB has been obtained over the spectral domain considered. The optimum value of the ER can be engineered by the appropriate choice of geometrical parameters, and the ER can reach a value of 100 dB, as the width of the subwavelength grating approaches the period. It is important to note that an ER value of ~150 dB could be realized simply by changing the thickness of the subwavelength grating. In addition, the fiber "meta-tip," integrating the proposed high-performance polarizer, also exhibits a value of 45 dB over the entire spectral domain. The design proposed may be easily scaled up to terahertz and other spectral ranges. As a result, it is proposed that a grating polarizer with ultrahigh ER over a broad bandwidth will be a promising candidate in the design of improved polarization selective devices, such as spectral filters and beam splitters.

ACKNOWLEDGMENTS

This work was supported by the National Natural Science Foundation of China (NSFC) (Grant Nos. 62275061 and 62175049), the Natural Science Foundation of Heilongjiang Province in China (Grant No. ZD2020F002), 111 project to the Harbin Engineering University (Grant No. B13015), and Fundamental Research Funds for the Central Universities (Grant No. 3072022TS2509).

AUTHOR DECLARATIONS

Conflict of Interest

The authors have no conflicts to disclose.

Author Contributions

Chunhua Qin: Investigation (equal); Resources (equal); Writing – original draft (equal). **Yiyuan Wang**: Formal analysis (equal); Software (equal); Writing – original draft (equal); Writing – review & editing (equal). **Ziying Liu**: Resources (equal); Software (equal); Writing – review & editing (equal). **Wenjia Li**: Supervision (equal); Writing – review & editing (equal). **Yuxiang Li**: Software (equal); Writing – review & editing (equal). **Ping Li**: Formal analysis (equal); Writing – review & editing (equal). **Zheng Zhu**: Funding acquisition (equal); Software (equal); Writing – review & editing (equal). **Chunying Guan**: Funding acquisition (equal); Writing – review & editing (equal). **Jinghui Shi**: Supervision (equal); Writing – review & editing (equal). **Kenneth T. V. Grattan**: Validation (equal); Writing – review & editing (equal).

DATA AVAILABILITY

The data that support the findings of this study are available from the corresponding author upon reasonable request.

REFERENCES

[1]S. Li, W. Jin, R. Xia, L. Li, and X. Wang, "Radiation correction method for infrared polarization imaging system with front-mounted polarizer," Opt. Express **24**(23), 26414–26430 (2016).

[2]H. Cheng, S. Q. Chen, P. Yu, J. X. Li, B. Y. Xie, Z. C. Li, and J. G. Tian, "Dynamically tunable broadband mid-infrared cross polarization converter based on graphene metamaterial," Appl. Phys. Lett. **103**(22), 223102 (2013).

[3]W. Cho, J. Hwang, S. Y. Lee, J. Park, N. Han, C. H. Lee, S. W. Kang, A. Urbas, J. O. Kim, Z. Ku, and J. J. Wie, "Highly sensitive and cost-effective polymeric-sulfur-based mid-wavelength infrared linear polarizers with tailored Fabry–Pérot resonance," Adv. Mater. **35**, 2209377 (2023).

[4]Y. Intaravanne and X. Chen, "Recent advances in optical metasurfaces for polarization detection and engineered polarization profiles," Nanophotonics **9**(5), 1003–1014 (2020).

[5]H. Cheng, X. Y. Wei, P. Yu, Z. C. Li, Z. Liu, J. J. Li, S. Q. Chen, and J. G. Tian, "Integrating polarization conversion and nearly perfect absorption with multifunctional metasurfaces," Appl. Phys. Lett. **110**(17), 171903 (2017).

[6]C. Caucheteur, T. Guo, and J. Albert, "Polarization-assisted fiber Bragg grating sensors: Tutorial and review," J. Lightwave Technol. **35**(16), 3311–3322 (2017).

[7]Z. Zhang, J. Gan, T. Yang, Y. Wu, Q. Li, S. Xu, and Z. Yang, "All-fiber mode-locked laser based on microfiber polarizer," Opt. Lett. **40**(5), 784–787 (2015).

[8]Q. Li, W. He, H. Deng, F. Y. Zhong, and Y. Chen, "High-performance reflection-type augmented reality 3D display using reflective polarizer," Opt. Express **29**(6), 9446–9453 (2021).

[9]J. H. Lee, J. Woong Yoon, M. Jin Jung, J. Kyun Hong, S. Ho Song, and R. Magnusson, "A semiconductor meta-surface with multiple functionalities: A polarizing beam splitter with simultaneous focusing ability," Appl. Phys. Lett. **104**(23), 233505 (2014).

[10]S. Wang, Z.-L. Deng, Y. Wang, Q. Zhou, X. Wang, Y. Cao, B.-O. Guan, S. Xiao, and X. Li, "Arbitrary polarization conversion dichroism meta-surfaces for all-in-one full Poincaré sphere polarizers," Light: Sci. Appl. **10**(1), 24 (2021).

[11]X. Wang, J. Li, X. Wang, Z. Tan, R. Chen, X. Deng, and Z. Wang, "Low-loss broadband transverse electric pass hybrid plasmonic fiber polarizers using metallic nanomaterials," ACS Appl. Mater. Interfaces **13**(12), 14718–14727 (2021).

[12]D. J. Broer, J. Lub, and G. N. Mol, "Wide-band reflective polarizers from cholesteric polymer networks with a pitch gradient," Nature **378**(6556), 467–469 (1995).

[13]A. Rahnama, T. Dadalyan, K. Mahmoud Aghdami, T. Galstian, and P. R. Herman, "In-fiber switchable polarization filter based on liquid crystal filled hollow-filament Bragg gratings," Adv. Opt. Mater. **9**(19), 2100054 (2021).

[14]I. Yamada, K. Takano, M. Hangyo, M. Saito, and W. Watanabe, "Terahertz wire-grid polarizers with micrometer-pitch Al gratings," Opt. Lett. **34**(3), 274–276 (2009).

[15]K. Takano, H. Yokoyama, A. Ichii, I. Morimoto, and M. Hangyo, "Wire-grid polarizer sheet in the terahertz region fabricated by nanoimprint technology," Opt. Lett. **36**(14), 2665–2667 (2011).

[16]K. J. Lee, J. Curzan, M. Shokooh-Saremi, and R. Magnusson, "Resonant wideband polarizer with single silicon layer," Appl. Phys. Lett. **98**(21), 211112 (2011).

[17]L. Y. Deng, J. H. Teng, L. Zhang, Q. Y. Wu, H. Liu, X. H. Zhang, and S. J. Chua, "Extremely high extinction ratio terahertz broadband polarizer using bilayer subwavelength metal wire-grid structure," Appl. Phys. Lett. **101**(1), 011101 (2012).

[18]Y. Zhao, M. A. Belkin, and A. Alù, "Twisted optical metamaterials for planarized ultrathin broadband circular polarizers," Nat. Commun. **3**(1), 870 (2012).

[19]B. Cheng, Y. X. Zou, H. X. Shao, T. Li, and G. F. Song, "Full-Stokes imaging polarimetry based on a metallic metasurface," Opt. Express **28**(19), 27324–27336 (2020).

[20]Z. Huang, E. P. J. Parrott, H. Park, H. P. Chan, and E. Pickwell-MacPherson, "High extinction ratio and low transmission loss thin-film terahertz polarizer with a tunable bilayer metal wire-grid structure," Opt. Lett. **39**(4), 793–796 (2014).

[21]K. J. Lee, J. Giese, L. Ajayi, R. Magnusson, and E. Johnson, "Resonant grating polarizers made with silicon nitride, titanium dioxide, and silicon: Design, fabrication, and characterization," Opt. Express **22**(8), 9271–9281 (2014).

[22]H. Kurosawa and S.-I. Inoue, "Enhanced extinction ratios of metasurface polarizers by surface-plasmon interference," J. Opt. Soc. Am. B **37**(3), 673–681 (2020).

[23]H. Hemmati, P. Bootpakdeetam, and R. Magnusson, "Metamaterial polarizer providing principally unlimited extinction," Opt. Lett. **44**(22), 5630 (2019).

[24]A. Basiri, X. Chen, J. Bai, P. Amrollahi, J. Carpenter, Z. Holman, C. Wang, and Y. Yao, "Nature-inspired chiral metasurfaces for circular polarization detection and full-Stokes polarimetric measurements," Light: Sci. Appl. **8**(1), 78 (2019).

[25]P. Bootpakdeetam, H. Hemmati, and R. Magnusson, "Cascaded metamaterial polarizers for the visible region," Opt. Lett. **45**(24), 6831–6834 (2020).

[26]H. Kurosawa, B. Choi, Y. Sugimoto, and M. Iwanaga, "High-performance meta-surface polarizers with extinction ratios exceeding 12000," Opt. Express **25**(4), 4446–4455 (2017).

[27]T. Siefke, S. Kroker, K. Pfeiffer, O. Puffky, K. Dietrich, D. Franta, I. Ohlídal, A. Szeghalmi, E. B. Kley, and A. Tünnermann, "Materials pushing the application limits of wire grid polarizers further into the deep ultraviolet spectral range," Adv. Opt. Mater. **4**(11), 1780–1786 (2016).

[28]T. Suzuki, M. Nagai, and Y. Kishi, "Extreme-sensitivity terahertz polarizer inspired by an anisotropic cut-through metamaterial," Opt. Lett. **41**(2), 325–328 (2016).

[29]J. H. Kang, H. S. Yun, H. I. Jang, J. H. Kim, J. H. Park, and J. Y. Lee, "Solution-processed aluminum nanogratings for wire grid polarizers," Adv. Opt. Mater. **6**(14), 1800205 (2018).

[30]Y. Chen, J. Gao, and X. Yang, "Direction-controlled bifunctional meta-surface polarizers," Laser Photonics Rev. **12**(12), 1800198 (2018).

[31]H. Kurosawa and S. Inoue, "Subwavelength high-performance polarizers in the deep ultraviolet region," Opt. Express **28**(8), 11652–11665 (2020).

[32]Z. Yan, C. Mou, H. Wang, K. Zhou, Y. Wang, W. Zhao, and L. Zhang, "All-fiber polarization interference filters based on 45°-tilted fiber gratings," Opt. Lett. **37**(3), 353–355 (2012).

[33]Q. Bao, H. Zhang, B. Wang, Z. Ni, C. H. Y. X. Lim, Y. Wang, D. Y. Tang, and K. P. Loh, "Broadband graphene polarizer," Nat. Photonics **5**(7), 411–415 (2011).

[34]R. Chu, C. Guan, J. Yang, Z. Zhu, P. Li, J. Shi, P. Tian, L. Yuan, and G. Brambilla, "High extinction ratio D-shaped fiber polarizers coated by a double graphene/PMMA stack," Opt. Express **25**(12), 13278–13285 (2017).

[35]J. F. Lu, Y. Dai, Q. Li, Y. L. Zhang, C. H. Wang, F. F. Pang, T. Y. Wang, and X. L. Zeng, "Fiber nanogratings induced by femtosecond pulse laser direct writing for in-line polarizer," Nanoscale **11**(3), 908–914 (2019).

[36]B. Yahyaei, O. Panahi, S. Malekmohamadi, M. Mousavi, M. Mardiha, and M. Kheyrollahi, "Novel in-line effective fiber polarizer based on chromium and gold nano metal films: Design and experiment," Laser Phys. **27**(1), 015101 (2017).

[37]X. Zhang, C. Wang, R. Yu, L. Xiao, X.-S. Zhu, and Y.-W. Shi, "Fiber polarizer based on selectively silver-coated large-core suspended-core fiber," Opt. Lett. **46**(10), 2429–2432 (2021).

[38]X. Wang, J. Lin, W. Sun, Z. Tan, R. Liu, and Z. Wang, "Polarization selectivity of the thin-metal-film plasmon-assisted fiber-optic polarizer," ACS Appl. Mater. Interfaces **12**(28), 32189–32196 (2020).

[39]Y. B. Lin, J. P. Guo, and R. G. Lindquist, "Demonstration of an ultra-wideband optical fiber inline polarizer with metal nano-grid on the fiber tip," Opt. Express **17**(20), 17849–17854 (2009).

[40]M. Vanek, J. Vanis, Y. Baravets, F. Todorov, J. Ctyroky, and P. Honzatko, "High-power fiber laser with a polarizing diffraction grating milled on the facet of an optical fiber," Opt. Express **24**(26), 30225–30233 (2016).

[41]W. Bai, M. H. Yang, J. X. Dai, H. H. Yu, G. P. Wang, and C. J. Qi, "Novel polyimide coated fiber Bragg grating sensing network for relative humidity measurements," Opt. Express **24**(4), 3230–3237 (2016).

[42]P. B. Johnson and R. W. Christy, "Optical constants of the noble metals," Phys. Rev. B **6**, 4370–4379 (1972).

[43]B. Cheng, L. Wang, Y. X. Zou, L. F. Lv, C. C. Li, Y. Xu, and G. F. Song, "Large bandwidth and high-efficiency plasmonic quarter-wave plate," Opt. Express **29**(11), 16939–16949 (2021).

[44]G. Soma, W. Yanwachirakul, T. Miyazaki, E. Kato, B. Onodera, R. Tanomura, T. Fukui, S. Ishimura, M. Sugiyama, Y. Nakano, and T. Tanemura, "Ultra-

broadband surface-normal coherent optical receiver with nanometallic polarizers," ACS Photonics **9**(8), 2842–2849 (2022).
[45]C. W. Moon, Y. Kim, and J. K. Hyun, "Active electrochemical high-contrast gratings as on/off switchable and color tunable pixels," Nat. Commun. **13**(1), 3391 (2022).
[46]Q. Cao and P. Lalanne, "Negative role of surface plasmons in the transmission of metallic gratings with very narrow slits," Phys. Rev. Lett. **88**(1–4), 057403 (2002).
[47]Z. W. Wang, J. L. Gong, A. M. Dong, and B. Cui, "Mechanism analyzation of the effects of grating parameters on polarization transmission of single-layer nanowire gratings," Proc. Inst. Mech. Eng., Part N **232**(1), 41–47 (2018).